BIOLOGICAL CHEMISTRY

10.1126/sciadv.1500137

Extension of the generic amyloid hypothesis to nonproteinaceous metabolite assemblies

Shira Shaham-Niv,[1] Lihi Adler-Abramovich,[1,2] Lee Schnaider,[1] Ehud Gazit[1,3]*

The accumulation of amyloid fibrils is the hallmark of several major human diseases. Although the formation of these supramolecular entities has previously been associated with proteins and peptides, it was later demonstrated that even phenylalanine, a single amino acid, can form fibrils that have amyloid-like biophysical, biochemical, and cytotoxic properties. Moreover, the generation of antibodies against these assemblies in phenylketonuria patients and the correlating mice model suggested a pathological role for the assemblies. We determine that several other metabolites that accumulate in metabolic disorders form ordered amyloid-like ultrastructures, which induce apoptotic cell death, as observed for amyloid structures. The formation of amyloid-like assemblies by metabolites implies a general phenomenon of amyloid formation, not limited to proteins and peptides, and offers a new paradigm for metabolic diseases.

INTRODUCTION

A plethora of degenerative disorders, including Alzheimer's disease, Parkinson's diseases, and type II diabetes, are associated with the formation of well-ordered amyloid fibrils (*1*–*6*). Pioneering work by Dobson and co-workers revealed that proteins that are not related to disease, such as the SH3 domain and myoglobin, can also form typical amyloid structures (*7*, *8*). After this, many other proteins unrelated to disease were shown to self-assemble to form these archetypal nanofibrils. It was therefore suggested that the amyloid conformation may actually represent a general form of backbone packing and a stable minimal energy arrangement for the organization of the polypeptide chain (*9*, *10*). Moreover, the toxicity of amyloid assemblies appeared to be a generic property of the formed structures, rather than as a disease-specific pathology, thus implying a common mechanism for the toxic effect (*11*).

Until recently, this visionary paradigm-shifting model for molecular association and energy landscape was limited to proteins and polypeptides (*12*). However, it was recently demonstrated that the single phenylalanine amino acid can form well-ordered amyloid-like fibrillar assemblies. These fibrils bind the amyloid-specific thioflavin T (ThT) and Congo red dyes. Moreover, the assemblies were found to have a significant cytotoxic effect allowing distinct immunogenicity, similar to amyloid deposits (*13*). In addition, single-crystal x-ray diffraction analysis of zwitterionic phenylalanine, under the condition in which it was found to form fibrillar assemblies, demonstrated a tight packing of the amino acid (*14*) in a pattern that resembles a β sheet secondary structure (Fig. 1A). This provided an important observation because conventional secondary structure evaluation methods such as circular dichroism and Fourier transform infrared spectroscopy are not applicable due to the absence of an amide chromophore. The observed formation of amyloid-like fibrils by phenylalanine was suggested to provide new mechanistic insights into the observed progression of pathology in phenylketonuria (PKU). Physiological accumulation of phenylalanine in body tissues, plasma, and urine is a characteristic of the PKU metabolic disorder (*15*). The cytotoxicity of the phenylalanine fibrils, which highly resembles that of amyloid fibrils, may provide an explanation for the mental retardation observed in PKU patients who do not maintain a restricted diet. The detection of phenylalanine assemblies in the brain of PKU model mice and individuals affected by the disorder supports this notion (Fig. 1A).

Metabolic disorders, such as PKU, are the result of cellular inability to perform critical biochemical reactions that involve various biosynthetic pathways. In the case of inborn error of metabolism, most disorders are due to the malfunction of single genes that encode for enzymes participating in metabolic processes, mainly in the conversion of various substances into processed products. In most of the disorders, abnormalities arise because of accumulation of metabolites, which are toxic or interfere with the normal function of cells and tissues. Unless these inherited dysfunctions are treated with a very strict diet, they may result in mental retardation and other developmental abnormalities. More than 50 metabolic disorders have been reported and described thus far, but because most of them are rare, occurring in less than 1 per 250,000 persons in most populations, a limited amount of targeted research, lacking in general mechanistic insights on these maladies, has been conducted. However, it is important to state that collectively, metabolic disorders constitute a very substantial part of pediatric genetic diseases. Because the molecular basis of tissue damage is poorly understood, it leaves the patients without any disease-modifying treatment (*15*). The formation of well-ordered assemblies by phenylalanine in the PKU patients and model animals was the first demonstration of amyloid formation by nonprotein entities. Here, we explored the possibility of a generic phenomenon in which other metabolites that accumulate in pathological states self-assemble to form amyloid-like apoptosis-inducing structures.

RESULTS

We initially composed a comprehensive list of enzymatic products that were found to accumulate in genetic inborn error of metabolism disorders (Fig. 1B) (*16*). Next, we explored possible conditions under which these soluble metabolites may undergo self-association. While attempting

[1]Department of Molecular Microbiology and Biotechnology, George S. Wise Faculty of Life Sciences, Tel Aviv University, Tel Aviv 69978, Israel. [2]Department of Oral Biology, The Goldschleger School of Dental Medicine, Tel Aviv Univeristy, Tel Aviv 69978, Israel. [3]Department of Materials Science and Engineering, Iby and Aladar Fleischman Faculty of Engineering, Tel Aviv University, Tel Aviv 69978, Israel.
*Corresponding author. E-mail: ehudg@post.tau.ac.il

to mimic physiological conditions, we dissolved the metabolites in phosphate-buffered saline (PBS) to reflect physiological pH and ionic strength. We first dissolved the metabolites at 90°C in physiological buffer to obtain a homogenous monomeric solution. This was followed by gradual cooling of the solution, which resulted in the formation of ultrastructures. Each metabolite was assayed at various concentrations to determine the conditions under which it forms ordered supramolecular entities. Several of the studied metabolites were found to form elongated and fibrillar structures with nanoscale order, including adenine, orotic acid, cystine (an amino acid formed by the oxidation of two cysteine molecules that covalently link via a disulfide bond), tyrosine, uracil, and phenylalanine (Fig. 2). Comprehensive analysis of the propensity for amyloid fibril formation, by all coded amino acids, in the context of peptides and proteins, had identified phenylalanine, cysteine, and tyrosine as residues with the highest aggregation potential (*17*, *18*). Therefore, it appears to be that the observed behavior of the various amino acids in the polypeptide chain may also be comparable as free amino acids.

We characterized the structure of the metabolite assemblies and examined whether they have ordered amyloid-like characteristics. For that purpose, we applied a set of biophysical assays to determine whether the hallmarks of amyloid are observed, including electron microscopy analysis and positive staining with Congo red (fig. S1) and ThT amyloid-specific dyes (Fig. 2) (*19*, *20*). Transmission electron microscopy (TEM) analysis of the metabolite assemblies displayed the appearance of typical

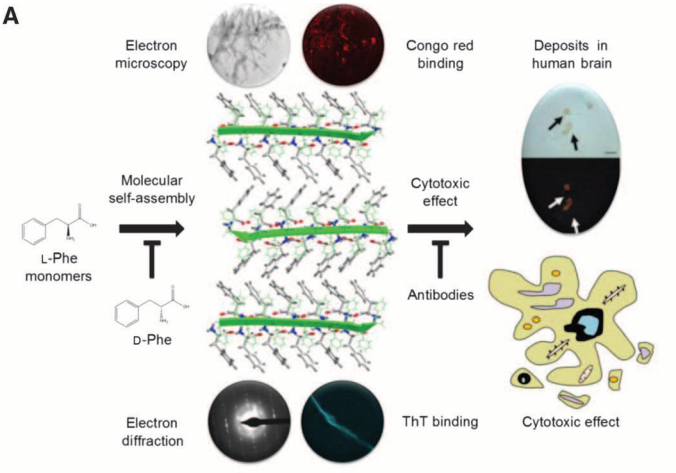

B

Metabolite	Disorder
Adenine	Adenine phosphoribosyltransferase deficiency
Argenine	Arginase deficiency
Cystine	Cystinuria, cystinosis
Glycine	Non-ketotic hyperglycinemia, D-glyceric aciduria, iminoglycinuria
Homogentisic acid	Alkaptonuria
Isoleucine	Maple syrup urine disease
Leucine	Maple syrup urine disease
Lysine	Saccharopinuria
Methionine	Hypermethioninemia
N-Acetyl aspartate	Canavan disease
Orotic acid	Ornithine transcarbamylase deficiency
Phenylalanine	Phenylketonuria
Proline	Hyperprolinemia, iminoglycinuria
Tryptophan	Hypertryptophanemia, Hartnup disease
Tyrosine	Tyrosinemia
Uracil	Ornithine transcarbamylase deficiency, dihydropyrimidine dehydrogenase deficiency
Uric acid	Gout, Lesch-Nyhan syndrome
Valine	Isobutyryl-CoA dehydrogenase deficiency, maple syrup urine disease

Fig. 1. The organization and assembly of metabolites into ordered structures. (**A**) L-Phenylalanine self-assembles into well-ordered amyloid-like assemblies with typical nanofibrillar dimensions as observed by electron microscopy, ordered electron diffraction pattern [modified from (*13*)], and binding to amyloid-specific dyes (ThT and Congo red). The crystal structure of zwitterionic phenylalanine represents the same molecular spacing as of a hypothetical polyphenylalanine stand (in green) and may be regarded as a supramolecular strand-like organization. The assemblies formed are cytotoxic, and their deposition could be observed in the brains of PKU patients. The self-assembly could be inhibited by the D-phenylalanine stereoisomer (*30*). The cytotoxic effect could be prevented by depletion with specific antibodies raised toward the supramolecular assemblies (*13*). (**B**) Overall review of genetic inborn error of metabolism disorders and their related accumulating metabolites.

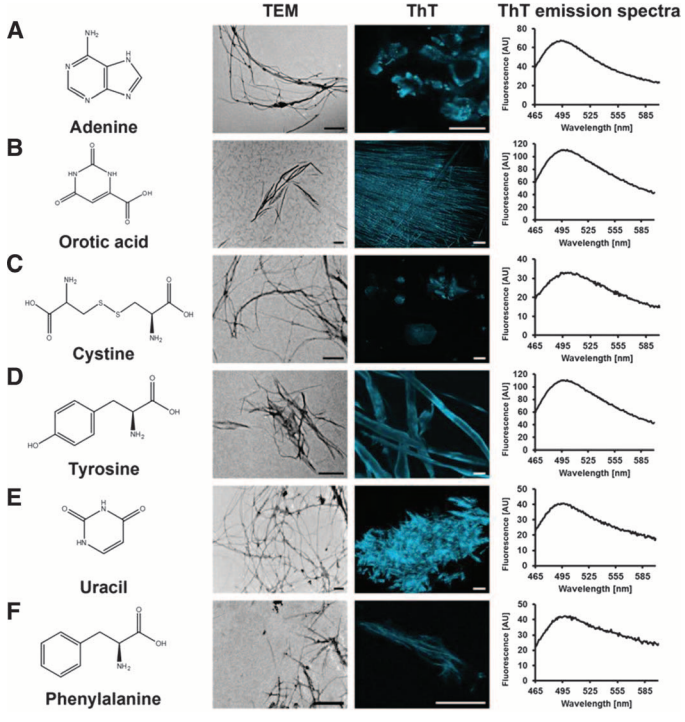

Fig. 2. Formation of amyloid-like structures by metabolite self-assembly. Skeletal formula, TEM micrographs of elongated metabolite fibrils, confocal fluorescence microscopy images of metabolite stained with ThT, and ThT fluorescence emission spectra images. All metabolites were dissolved at 90°C in PBS. Columns from left to right (as indicated above): TEM micrographs. Scale bars, 500 nm. Confocal microscopy images were taken immediately after the addition of the ThT reagent at a 1:1 ratio with the metabolites, with excitation and emission wavelengths of 458 and 485 nm, respectively. Scale bars, 20 μm. ThT emission spectra (excitation at 430 nm) were collected for each of the metabolites. Aged samples of each metabolite were added to 40 μM ThT in PBS to a final concentration of 20 μM ThT. (**A**) Adenine—TEM (1 mg/ml), ThT microscopy (4 mg/ml) and spectra (2 mg/ml). (**B**) Orotic acid—TEM (1 mg/ml), ThT microscopy and spectra (2 mg/ml). (**C**) Cystine—TEM (1 mg/ml), ThT microscopy and spectra (2 mg/ml). (**D**) Tyrosine—TEM (1 mg/ml), ThT microscopy and spectra (4 mg/ml). (**E**) Uracil—TEM (5 mg/ml), ThT microscopy and spectra (10 mg/ml). (**F**) Phenylalanine—TEM (2 mg/ml), ThT microscopy and spectra (4 mg/ml). AU, arbitrary units.

amyloid fibrils. All assemblies formed are characterized by very similar biophysical properties and are all able to self-assemble into curved and twisted fibers, which differ in their length (Fig. 2, TEM column), with the diameter of the fibers varying between 6 and 50 nm (table S1). For further examination of the amyloid-like nature of the metabolite assemblies, we used ThT and Congo red fluorescence assays. These reagents change their fluorescence properties upon binding to ordered amyloid-like structures that could later be monitored by fluorescence microscopy. Indeed, these metabolite assemblies presented a typical change in the fluorescence signal as observed with the binding of ThT and Congo red to amyloid fibrils (Fig. 2 and fig. S1). In addition, the metabolite amyloid-like fibers present spectra correlating to those of typical polypeptide amyloid fibrils and exhibit the amyloid common emission signal at 480 nm, when excited at 450 nm (Fig. 2 and fig. S2).

Amyloid diseases represent a large group of pathological conditions that are characterized by the accumulation of fibrillar deposits located in the intracellular or extracellular milieu, where they lead to noted cell death in various organs and tissues (*4*, *21*, *22*). Here, we explored whether the metabolite assemblies, as described above, can display a cytotoxic effect, similar to that of classical amyloid fibrils. We examined a set of metabolite concentrations (0.2, 2, and 4 mg/ml) for the metabolite assemblies, except orotic acid, which was not soluble in a concentration of 4 mg/ml, and thus, a concentration of 1 mg/ml was tested instead. The above-stated concentrations of the metabolites were added to the cultured SH-SY5Y cell line, which is often used as an in vitro model of neuronal function.

The metabolite assemblies displayed a dose-dependent cytotoxic effect on the cells, as indicated by the 2,3-bis-(2-methoxy-4-nitro-5-sulphophenyl)-2*H*-tetrazolium-5-carboxanilide (XTT) cell viability assay (Fig. 3, A to E). Metabolites in medium alone served as a control, showing that the change in the absorbance was due to the change in cell viability and was not affected by the structures formed by the metabolites. For this reason, cystine assemblies could not be examined using this assay, because they absorb at the same wavelength as the XTT reagent, thus affecting the absorbance even without the presence of any cells. Additionally, we were interested in determining the concentrations that resulted in ~50% reduction in cell viability, and thus, a uracil concentration of 10 mg/ml was examined as well, because lower concentrations did not trigger such an effect. The highest concentration of adenine had the most cytotoxic effect out of all tested metabolites, inducing a decrease in cell viability to about 33% (Fig. 3A). The highest concentration of the other investigated metabolites resulted in a decrease in cell viability to about 50% (Fig. 3, B to E). To examine whether the observed toxic effect was not an outcome of osmotic stress or any other colligative properties, but indeed due to the metabolite structures, the alanine amino acid was used as a negative control. Alanine was not reported to accumulate in any metabolic disorder, and when analyzed under the same set of concentrations and conditions, no structure formation was observed. Moreover, alanine did not demonstrate any toxic effect even in the highest concentration of 10 mg/ml (Fig. 3F), supporting the notion that the toxic effect was due to the formation of supramolecular metabolite structures.

To explore whether the metabolite assemblies trigger the process of apoptotic cell death, as was reported for amyloid fibrils (*22*–*28*), we used the annexin V and propidium iodide (PI) apoptosis assay. The effect of the metabolites was studied using the same SH-SY5Y cell model, at a concentration that was found to result in about 50% decrease in cell viability by the XTT cell viability assay. Cystine was not soluble in a concentration higher than 2 mg/ml and thus was examined at this concentration. The tested metabolite assemblies induced a clear apoptotic effect on cultured cells, as observed in all analyses as the major route for cell toxicity (Fig. 4A). Cystine had the strongest apoptotic effect resulting in 62% cell apoptosis (Fig. 4C), phenylalanine addition resulted in 55% cell apoptosis (Fig. 4F), whereas adenine tyrosine and uracil triggered 40 to 50% cell apoptosis (Fig. 4, B, D, and G). Orotic acid demonstrated a slightly lower effect causing about 30% cell apoptosis (Fig. 4E). The negative control, using alanine as before, did not present any apoptotic response on examined cells (Fig. 4H).

Both assays imply that the metabolite assemblies not only present a cytotoxic effect, like amyloid structures, but also induce programmed cell death, which is consistent with the mechanism suggested for amyloids (*28*). Results of the negative control, the amino acid alanine, imply that it is not the concentration of metabolite monomers but rather the presence of the amyloid-like metabolites assemblies that causes the toxic effect. In addition to the use of alanine as a control, to rule out the possibility that the cytotoxic effect is caused by the metabolites themselves rather than their amyloid-like structures, exhaustive centrifugation of each sample was carried out to pellet aggregated forms. The resulting supernatant was also used to treat the SH-SY5Y neuronal cell model, which also underwent cytotoxicity analysis using XTT cell viability assay and annexin V and PI apoptosis assay (fig. S3). The great majority of monomeric metabolites displayed almost no effect on cell viability, whereas adenine itself did cause a slight decrease in cell viability (fig. S3, A and B), yet markedly less severe than that of its aggregative state

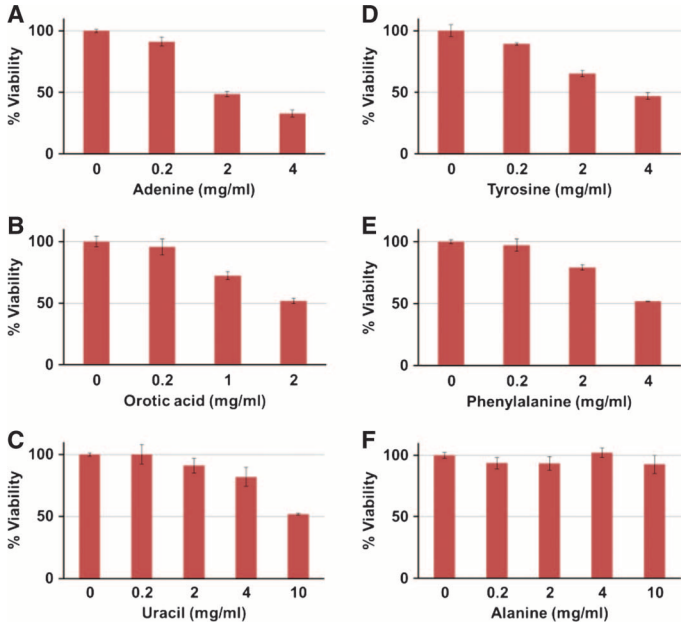

Fig. 3. Cytotoxicity of the metabolite assemblies as determined by XTT assay. Metabolites were dissolved at 90°C in cell medium followed by gradual cooling of the solution. The control (zero concentration of metabolites) reflects medium with no metabolites, which was treated in the same manner. Treated SH-SY5Y cells were incubated with medium containing metabolites for 6 hours, following the addition of the XTT reagent. After 2.5 hours of incubation, absorbance was determined at 450 nm. The results represent three biological repeats; error bars represent 95% confidence interval ($P < 0.01$). (**A**) Adenine. (**B**) Orotic acid. (**C**) Uracil. (**D**) Tyrosine. (**E**) Phenylalanine. (**F**) Alanine.

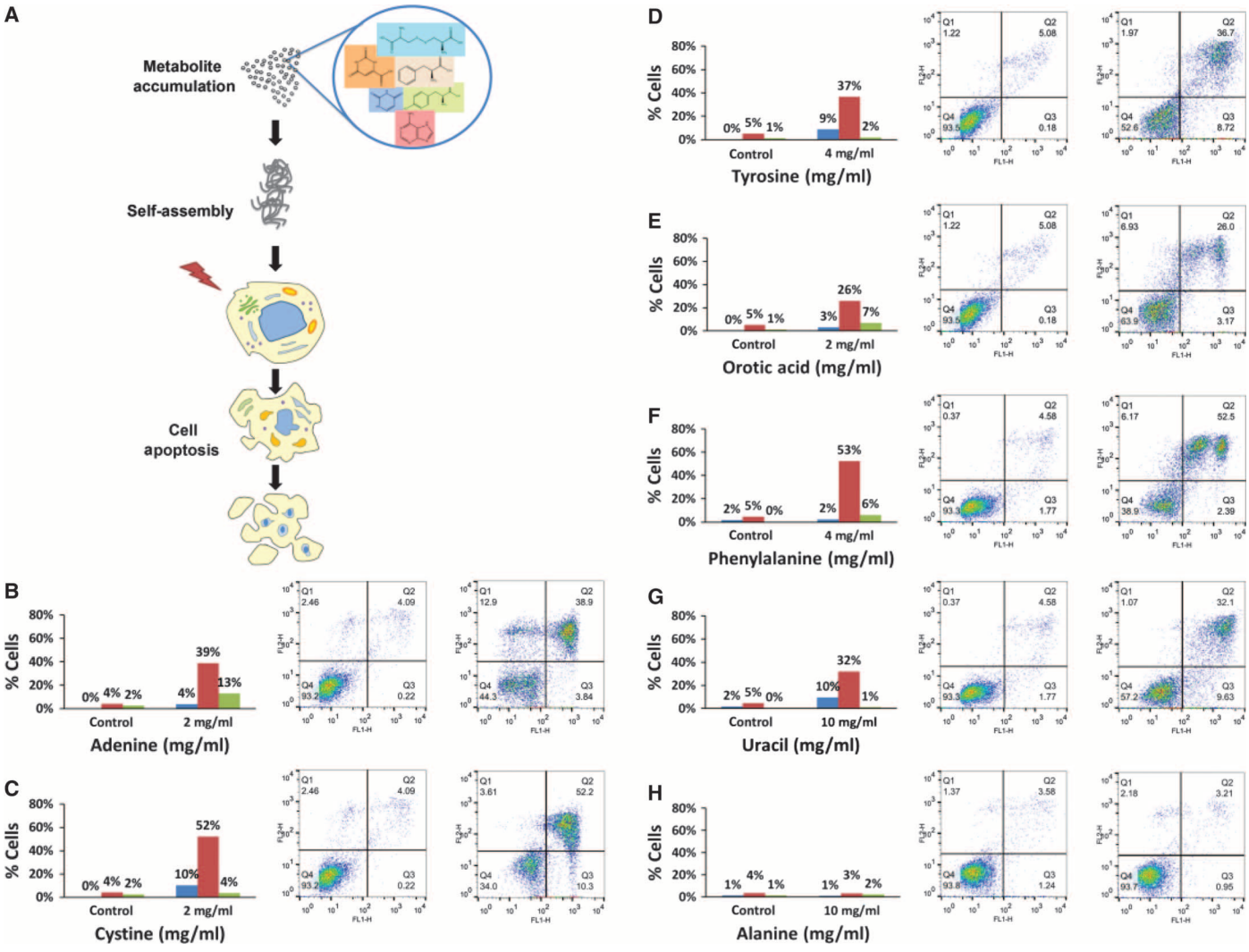

Fig. 4. Apoptotic activity of the assemblies studied by annexin V and PI assay. Metabolites were dissolved at 90°C in cell medium followed by gradual cooling of the solution. The control reflects medium with no metabolites, which was treated in the same manner. Treated SH-SY5Y cells were incubated with medium containing metabolites in the stated concentrations for 24 hours. Control cells were incubated with medium without any addition of metabolites. After incubation, annexin V–FITC (fluorescein isothiocyanate) and PI reagents were added to the cell cultures following the measurement of the cell samples by flow cytometry using single laser emitting excitation light at 488 nm. Early apoptosis is represented in blue, late apoptosis in red, and necrosis in green. (**A**) Schematic depiction of metabolites that self-assemble into amyloid-like structures, which triggers apoptotic effect. (**B**) Adenine. (**C**) Cystine. (**D**)Tyrosine. (**E**) Orotic acid. (**F**) Phenylalanine. (**G**) Uracil. (**H**) Alanine.

(Figs. 3A and 4B). Together, these results rule out the possibility that the soluble metabolites trigger cell toxicity and confirm that the toxic element is the amyloid-like structures formed by the metabolites.

Because of the fact that these inborn errors of metabolism type of disorders are rare, not much is known about the pathological concentrations of the disorder-related metabolites in patient's plasma. In the case of phenylalanine, we have used higher concentrations than the known pathological concentration in PKU patients in our analysis in an attempt to mimic the progression of the disease at in vitro settings in shorter periods of time. In addition, the high concentrations of metabolites can be correlated to the local high concentrations that accumulate in a specific tissue or organ, as often happens in pathologic states. In a similar manner, whereas in Alzheimer's disease the cerebral concentration of the β-amyloid polypeptide is lower than 10 nM, micromolar concentration ranges are used in experimental toxicity studies (*29*).

DISCUSSION

To summarize, we found that similar to the previously reported formation of amyloid-like assemblies by the phenylalanine amino acid, several other metabolites also assemble into ordered entities. Biophysical characterization of these assemblies revealed that all assembled ultrastructures formed by the various metabolites present amyloidogenic properties shown by electron microscopy and ThT and Congo red assays. Not only do these metabolites self-assemble into supramolecular

amyloid-like fibrillar structures, they also demonstrate a clear apoptotic effect on neuronal model cells. Thus, the mechanism as identified in PKU may represent a much more extensive paradigm for metabolic disorders. A mechanistic understating of the assembly process of metabolites and the structural rules for assembly could lead to the development of specific small molecular inhibitors of these toxic assemblies, which may also resemble those found in the case of amyloid aggregation therapeutic agents. Such insights should enable specific directed drug design, which may present a new innovational approach of treatment for these metabolic disorders.

MATERIALS AND METHODS

Materials

Metabolites were purchased from Sigma (alanine, cystine, orotic acid, phenylalanine, and tyrosine purity ≥98; adenine and uracil purity ≥99). Fresh stock solutions were prepared by dissolving the metabolites at 90°C in PBS or Dulbecco's modified Eagle's medium (DMEM)/Nutrient Mixture F12 (Ham's) (1:1) (Biological Industries) at various concentrations ranging from 0.2 to 10 mg/ml, followed by gradual cooling of the solution.

Transmission electron microscopy

Metabolites were dissolved at 90°C in PBS at various concentrations ranging from 1 to 5 mg/ml, followed by gradual cooling of the solution. A 10-μl aliquot of this solution was placed on 400-mesh copper grids. After 1 min, excess fluids were removed. Samples were viewed using a JEOL 1200EX electron microscope operating at 80 kV. Calculating the diameter of metabolite amyloidal fibers was done by measuring five fibers from three different images of each metabolite.

Congo red fluorescence assay

Metabolites were dissolved at 90°C in PBS at various concentrations ranging from 2 to 10 mg/ml, followed by gradual cooling of the solution. A 10-μl aliquot of the solution was allowed to dry on a glass microscope slide at room temperature. Staining was performed by the addition of 10 μl of Congo red staining solution [5 mM phosphate, 150 mM NaCl (pH 7.5), and saturated amount Congo red], which was also allowed to dry at room temperature. The stained samples were visualized using a fluorescence microscope (Nikon Eclipse TI, inverted) at excitation and emission wavelengths of 513 to 556 nm and 570 to 613 nm, respectively.

ThT staining and confocal laser microscopy imaging

Metabolites were dissolved at 90°C in PBS at various concentrations ranging from 2 to 10 mg/ml, followed by gradual cooling of the solution. ThT solution (10 μl, 2 mM, PBS 1×) was mixed with 10 μl of the metabolite solution and placed on a glass microscope slide. The stained samples were visualized using an LSM 510 confocal laser scanning microscope (Carl Zeiss) at excitation and emission wavelengths of 458 and 485 nm, respectively.

ThT fluorescence emission spectra and endpoint emission

Metabolites were dissolved at 90°C in PBS to the following concentrations: phenylalanine (4 mg/ml), tyrosine (4 mg/ml), orotic acid (2 mg/ml), uracil (10 mg/ml), cystine (2 mg/ml), and adenine (2 mg/ml), followed by gradual cooling of the solution. Aged samples of each metabolite were then added to 40 μM ThT in PBS to a final concentration of 20 μM ThT. ThT fluorescence emission spectra over 465 and 600 nm (excitation at 430 nm) as well as ThT emission at 480 nm (excitation at 450 nm) were collected via the Tecan Infinite M200 PRO Series fluorescent microplate reader.

Cell cytotoxicity experiments

SH-SY5Y cell line (2×10^5 cells/ml) were cultured in 96-well tissue microplates (100 μl per well) and allowed to adhere overnight at 37°C. Metabolites were dissolved at 90°C in DMEM/Nutrient Mixture F12 (Ham's) (1:1) (Biological Industries) at various concentrations ranging from 0.2 to 10 mg/ml, followed by gradual cooling of the solution. Each plate was divided, and only half of it was plated with cells. The negative control, represented by zero, was prepared as medium with no metabolites, which was treated in the same manner. Medium (100 μl) with or without metabolites was added to each well. After incubation for 6 hours at 37°C, cell viability was evaluated using the XTT cell proliferation assay kit (Biological Industries) according to the manufacturer's instructions. Briefly, 100 μl of the activation reagent was added to 5 ml of the XTT reagent, followed by the addition of 100 μl of activated XTT solution to each well. After 2.5 hours of incubation at 37°C, color intensity was measured using an enzyme-linked immunosorbent assay (ELISA) microplate reader at 450 and 630 nm. Results are presented as means ± SEM. Each experiment was repeated three times.

Flow cytometry for apoptosis studies

Metabolites were dissolved at 90°C in DMEM/Nutrient Mixture F12 (Ham's) (1:1) (Biological Industries) at various concentrations ranging from 2 to 10 mg/ml, followed by gradual cooling of the solution. SH-SY5Y cells were seeded at 2×10^5 per well in six-well plates and were allowed to adhere overnight, followed by incubation with medium containing metabolites for 24 hours. Control cells were incubated with medium that was treated in the same manner without any addition of metabolites. The apoptotic effect was evaluated using the MEBCYTO Apoptosis kit (MBL International), according to the manufacturer's instructions. Briefly, the adherent cells were trypsinized, detached, and combined with floating cells from the original growth medium. They were then centrifuged and washed once with PBS and once with binding buffer. Cells were incubated with annexin V–FITC and PI for 15 min in the dark, then resuspended in 400 μl of binding buffer, and analyzed by flow cytometry using a single laser emitting excitation light at 488 nm. Data from at least 10^4 cells were acquired using BD FACSort and the CellQuest software (BD Biosciences). Analyses were done with FlowJo software (TreeStar, version 14). Each experiment was repeated three times.

Sedimentation of metabolite soluble form

Metabolites were dissolved at 90°C in DMEM/Nutrient Mixture F12 (Ham's) (1:1) (Biological Industries) at various concentrations ranging from 2 to 10 mg/ml, followed by gradual cooling of the solution. Next, metabolite samples were centrifuged at 20,000*g* for 1 hour at 4°C. The control reflects medium with no metabolites, which was treated in the same manner. Treated SH-SY5Y cells were incubated with the resulting supernatant medium that contained the soluble form of the metabolites and were further analyzed using XTT cell viability assay and annexin V–FITC and PI apoptosis assay as was previously presented.

SUPPLEMENTARY MATERIALS

Supplementary material for this article is available at http://advances.sciencemag.org/cgi/content/full/1/7/e1500137/DC1

Table S1. Diameter of metabolite amyloidal fibers.

Fig. S1. Fluorescence microscopy images of metabolite stained with Congo red.

Fig. S2. Endpoint ThT emission.

Fig. S3. Cytotoxicity of the metabolites in their soluble form as determined by XTT assay and annexin V and PI assay.

REFERENCES AND NOTES

1. T. P. Knowles, M. Vendruscolo, C. M. Dobson, The amyloid state and its association with protein misfolding diseases. *Nat. Rev. Mol. Cell Biol.* **15**, 384–396 (2014).
2. D. Eisenberg, M. Jucker, The amyloid state of proteins in human diseases. *Cell* **148**, 1188–1203 (2012).
3. A. Aguzzi, T. O'Connor, Protein aggregation diseases: Pathogenicity and therapeutic perspectives. *Nat. Rev. Drug Discov.* **9**, 237–248 (2010).
4. C. A. Ross, M. A. Poirier, Protein aggregation and neurodegenerative disease. *Nat. Med.* **10**, S10–S17 (2004).
5. R. N. Rambaran, L. C. Serpell, Amyloid fibrils: Abnormal protein assembly. *Prion* **2**, 112–117 (2008).
6. A. Kapurniotu, Shedding light on Alzheimer's β-amyloid aggregation with chemical tools. *ChemBioChem* **13**, 27–29 (2012).
7. J. I. Guijarro, M. Sunde, J. A. Jones, I. D. Campbell, C. M. Dobson, Amyloid fibril formation by an SH3 domain. *Proc. Natl. Acad. Sci. U.S.A.* **95**, 4224–4228 (1998).
8. M. Fändrich, M. A. Fletcher, C. M. Dobson, Amyloid fibrils from muscle myoglobin. *Nature* **410**, 165–166 (2001).
9. F. Chiti, C. M. Dobson, Amyloid formation by globular proteins under native conditions. *Nat. Chem. Biol.* **5**, 15–22 (2009).
10. E. Gazit, The "correctly folded" state of proteins: Is it a metastable state? *Angew. Chem. Int. Ed.* **41**, 257–259 (2002).
11. M. Bucciantini, E. Giannoni, F. Chiti, F. Baroni, L. Formigli, J. Zurdo, N. Taddei, G. Ramponi, C. M. Dobson, M. Stefani, Inherent toxicity of aggregates implies a common mechanism for protein misfolding diseases. *Nature* **416**, 507–511 (2002).
12. T. Eichner, S. E. Radford, A diversity of assembly mechanisms of a generic amyloid fold. *Mol. Cell* **43**, 8–18 (2011).
13. L. Adler-Abramovich, L. Vaks, O. Carny, D. Trudler, A. Magno, A. Caflisch, D. Frenkel, E. Gazit, Phenylalanine assembly into toxic fibrils suggests amyloid etiology in phenylketonuria. *Nat. Chem. Biol.* **8**, 701–706 (2012).
14. E. Mossou, S. C. Teixeira, E. P. Mitchell, S. A. Mason, L. Adler-Abramovich, E. Gazit, V. T. Forsyth, The self-assembling zwitterionic form of L-phenylalanine at neutral pH. *Acta Crystallogr. C Struct. Chem.* **70**, 326–331 (2014).
15. D. Ferrier, R. Harvey, *Lippincott's Illustrated Reviews: Biochemistry* (Lippincott Williams & Wilkins, Philadelphia, PA, 2014).
16. D. Valle, A. L. Beudet, B. Vogelstein, K. W. Kinzler, S. E. Antonarakis, A. Ballabio, K. M. Gibson, G. Mitchell, Eds., *The Online Metabolic and Molecular Bases of Inherited Disease* (McGraw-Hill, New York, 2014).
17. A. P. Pawar, K. F. Dubay, J. Zurdo, F. Chiti, M. Vendruscolo, C. M. Dobson, Prediction of "aggregation-prone" and "aggregation-susceptible" regions in proteins associated with neurodegenerative diseases. *J. Mol. Biol.* **350**, 379–392 (2005).
18. P. W. Frederix, G. G. Scott, Y. M. Abul-Haija, D. Kalafatovic, C. G. Pappas, N. Javid, N. T. Hunt, R. V. Ulijn, T. Tuttle, Exploring the sequence space for (tri-)peptide self-assembly to design and discover new hydrogels. *Nat. Chem.* **7**, 30–37 (2014).
19. M. Biancalana, S. Koide, Molecular mechanism of Thioflavin-T binding to amyloid fibrils. *Biochim. Biophys. Acta* **1804**, 1405–1412 (2010).
20. R. P. Linke, Highly sensitive diagnosis of amyloid and various amyloid syndromes using Congo red fluorescence. *Virchows Arch.* **436**, 439–448 (2000).
21. L. Milanesi, T. Sheynis, W. F. Xue, E. V. Orlova, A. L. Hellewell, R. Jelinek, E. W. Hewitt, S. E. Radford, H. R. Saibil, Direct three-dimensional visualization of membrane disruption by amyloid fibrils. *Proc. Natl. Acad. Sci. U.S.A.* **109**, 20455–20460 (2012).
22. S. Grudzielanek, A. Velkova, A. Shukla, V. Smirnovas, M. Tatarek-Nossol, H. Rehage, A. Kapurniotu, R. Winter, Cytotoxicity of insulin within its self-assembly and amyloidogenic pathways. *J. Mol. Biol.* **370**, 372–384 (2007).
23. D. T. Loo, A. Copani, C. J. Pike, E. R. Whittemore, A. J. Walencewicz, C. W. Cotman, Apoptosis is induced by β-amyloid in cultured central nervous system neurons. *Proc. Natl. Acad. Sci. U.S.A.* **90**, 7951–7955 (1993).
24. F. M. LaFerla, B. T. Tinkle, C. J. Bieberich, C. C. Haudenschild, G. Jay, The Alzheimer's Aβ peptide induces neurodegeneration and apoptotic cell death in transgenic mice. *Nat. Genet.* **9**, 21–30 (1995).
25. T. Nakagawa, H. Zhu, N. Morishima, E. Li, J. Xu, B. A. Yankner, J. Yuan, Caspase-12 mediates endoplasmic-reticulum-specific apoptosis and cytotoxicity by amyloid-β. *Nature* **403**, 98–103 (2000).
26. Y. P. Li, A. F. Bushnell, C. M. Lee, L. S. Perlmutter, S. K. F. Wong, β-Amyloid induces apoptosis in human-derived neurotypic SH-SY5Y cells. *Brain Res.* **738**, 196–204 (1996).
27. F. G. Gervais, D. Xu, G. S. Robertson, J. P. Vaillancourt, Y. Zhu, J. Huang, A. LeBlanc, D. Smith, M. Rigby, M. S. Shearman, E. E. Clarke, H. Zheng, L. H. Van Der Ploeg, S. C. Ruffolo, N. A. Thornberry, S. Xanthoudakis, R. J. Zamboni, S. Roy, D. W. Nicholson, Involvement of caspases in proteolytic cleavage of Alzheimer's amyloid-β precursor protein and amyloidogenic Aβ peptide formation. *Cell* **97**, 395–406 (1999).
28. Y. Bram, A. Frydman-Marom, I. Yanai, S. Gilead, R. Shaltiel-Karyo, N. Amdursky, E. Gazit, Apoptosis induced by islet amyloid polypeptide soluble oligomers is neutralized by diabetes-associated specific antibodies. *Sci. Rep.* **4**, 4267 (2014).
29. S. Lesné, M. T. Koh, L. Kotilinek, R. Kayed, C. G. Glabe, A. Yang, M. Gallagher, K. H. Ashe, A specific amyloid-β protein assembly in the brain impairs memory. *Nature* **440**, 352–357 (2006).
30. V. Singh, R. K. Rai, A. Arora, N. Sinha, A. K. Thakur, Therapeutic implication of L-phenylalanine aggregation mechanism and its modulation by D-phenylalanine in phenylketonuria. *Sci. Rep.* **4**, 3875 (2014).

Acknowledgments: We thank A. Barbul for confocal microscopy analysis, O. Sagi-Assif for the fluorescence-activated cell sorting analysis, V. Holdengreber for help with TEM analysis, and members of the Gazit laboratory for helpful discussions. All data described in the paper are presented in this report and in the Supplementary Materials. **Author contributions:** S.S.-N., L.A.-A., and E.G. conceived and designed the experiments. S.S.-N. and L.S. planned and performed the experiments. S.S.-N., L.A.-A., L.S., and E.G. wrote the paper. All authors discussed the results and commented on the manuscript. **Competing interests:** The authors declare that they have no competing interests.

Submitted 12 February 2015
Accepted 25 June 2015
Published 14 August 2015
10.1126/sciadv.1500137

Citation: S. Shaham-Niv, L. Adler-Abramovich, L. Schnaider, E. Gazit, Extension of the generic amyloid hypothesis to nonproteinaceous metabolite assemblies. *Sci. Adv.* **1**, e1500137 (2015).

Extension of the generic amyloid hypothesis to nonproteinaceous metabolite assemblies
Shira Shaham-Niv, Lihi Adler-Abramovich, Lee Schnaider and Ehud Gazit (August 14, 2015)
Sci Adv 2015, 1:.
doi: 10.1126/sciadv.1500137